HHS Public Access

Author manuscript

Nat Methods. Author manuscript; available in PMC 2015 September 01.

Published in final edited form as:

Nat Methods. 2015 March ; 12(3): 195–198. doi:10.1038/nmeth.3261.

Ratiometric biosensors based on dimerization-dependent fluorescent protein exchange

Yidan Ding[1], **Jiao Li**[2], **Jhon Ralph Enterina**[1], **Yi Shen**[1], **Issan Zhang**[3], **Paul H. Tewson**[4], **Gary C. H. Mo**[5], **Jin Zhang**[5], **Anne Marie Quinn**[4], **Thomas E. Hughes**[4,6], **Dusica Maysinger**[3], **Spencer C. Alford**[1,7], **Yan Zhang**[2], and **Robert E. Campbell**[1]

[1]Department of Chemistry, University of Alberta, Edmonton, Alberta, Canada

[2]State Key Laboratory of Biomembrane and Membrane Biotechnology, College of Life Sciences, PKU (Peking University)-IDG (International Data Group)/McGovern Institute for Brain Research, Peking University, Beijing, China

[3]Department of Pharmacology and Therapeutics, McGill University, Montreal, Quebec, Canada

[4]Montana Molecular, Bozeman, Montana, United States of America

[5]Department of Pharmacology and Molecular Sciences, The Johns Hopkins University School of Medicine, Baltimore, Maryland, United States of America

[6]Department of Cell Biology and Neuroscience, Montana State University, Bozeman, Montana, United States of America

[7]Department of Bioengineering, Stanford University, Stanford, California, United States of America

Abstract

We have developed a versatile new class of genetically encoded fluorescent biosensor based on reversible exchange of the heterodimeric partners of green and red dimerization dependent

Correspondence should be addressed to R.E.C. (robert.e.campbell@ualberta.ca).

Accession codes. GenBank, Addgene: KF976774, 50835; KF976776, 50840; KM979348, 60972; KM979349, 60973; KF976775, 50836; KF976777, 50842; KF976778, 50843; KF976779, 50849; KF976780, 50852; KP030819, 61017; KP030818, 36294; KP030820, 61018; KP030822, 61020; KP030821, 61019; KP030816, 36292; KP030817, 36293; KM891584, 60886; KM891581, 60883; KM891582, 60884; KM891585, 60887; KM891583, 60885; KP001564, 60936; KP001565, 60937; KM979350, 60974. See Supplementary Table 1 for full details.

Note: Supplementary Information and Source Data files are available in the online version of the paper.

Author Contributions: Y.D., J.Z., P.H.T., A.M.Q., T.E.H., D.M., S.C.A., Y.Z., and R.E.C. conceived and designed experiments. Y.D. assembled all constructs except for the PIP_2, PKA, and ERK biosensors, and performed imaging of all caspase-3, -8, and -9 biosensors and the three-polypeptide Ca^{2+} biosensor. J.L. performed imaging with the caspase-3 biosensor in neurons. J.R.E. determined heterodimer affinities *in vitro*. Y.S. performed imaging of the single-polypeptide Ca^{2+} biosensor. I.Z. performed imaging of the caspase-1 biosensor. P.H.T. assembled and performed imaging of the PIP_2 and PKA biosensors. G.C.H.M. assembled and performed imaging of the ERK biosensor. All authors were involved in data analysis, and Y.D., J.Z., T.E.H., D.M., S.C.A., Y.Z., and R.E.C. wrote the manuscript.

Competing Financial Interests: The corresponding author, in partnership with the Alberta Glycomics Centre and the University of Alberta, has filed Canadian and US patent applications that describe the research in this manuscript. P.H.T., A.M.Q., and T.E.H. are employed by Montana Molecular, a for-profit company that develops genetically-encoded fluorescent protein sensors. This does not alter the authors' adherence to all of the *Nature Methods* policies on sharing data and materials presented in this manuscript.

fluorescent proteins (ddFPs). This strategy has been used to construct both intermolecular and intramolecular ratiometric biosensors for qualitative imaging of caspase activity, Ca^{2+} concentration dynamics, and other second messenger signaling activities.

Strategies for converting fluorescent proteins (FPs) into active biosensors of intracellular biochemistry are few in number and are technically challenging. The three most common methods are: Förster resonance energy transfer (FRET) between two different hues of FP[1,2]; bimolecular complementation of a split FP[3]; and engineering of a single FP to respond to an analyte of interest[4,5]. Each method has distinct advantages and disadvantages that make it applicable to a particular range of biosensing applications that would be impractical with the other technologies. In an effort to expand the range of biosensor design strategies and applications, we recently introduced dimerization-dependent fluorescent protein (ddFP) technology as a fourth option[6,7]. A ddFP is a pair of quenched or non-fluorescent FP-derived monomers that can associate to form a fluorescent heterodimer. One of the monomers (copy A) contains a chromophore that is quenched in the monomeric state. The second monomer (copy B) does not form a chromophore and only acts to substantially increase the fluorescence of copy A upon formation of the AB heterodimer. In the green and red fluorescent versions of ddFP, the A copies are referred to as GA and RA, respectively. We previously reported variants of B optimized to pair with either GA or RA, but later discovered that the B variants can interchangeably complement both GA and RA (Supplementary Fig. 1).

The realization that GA and RA could compete for binding to the same B variant led us to conceive of the Fluorescent Protein eXchange (FPX) biosensor design strategy (Fig. 1a). We reasoned that ratiometric fluorescent changes could be achieved through the exchange of one ddFP monomer between two complementary ddFP binding partners in response to a change in protein-protein interactions. While either the A or the B copy could be exchanged (i.e., between two different B or A copies, respectively), B copy exchange is the preferred implementation since this would result in a ratiometric change from red-to-green (or vice versa) fluorescence.

To determine if the FPX strategy was feasible, we constructed the gene encoding GA-DEVD-B, where DEVD represented the caspase-3 substrate sequence Asp-Glu-Val-Asp[2], and co-expressed it with RA in cultured mammalian cells (Fig. 1b). In this design, the green fluorescence should be initially bright due to the linkage of GA to the B copy. Upon cleavage, the B copy would be free to exchange with the free RA protein and the red fluorescence would increase as green fluorescence decreased. Indeed, cells stimulated to undergo apoptosis stochastically exhibited the expected change in fluorescence (Fig. 1c and Supplementary Movie 1), with red-to-green ratio changes of approximately 8-fold (Fig. 1d). Performing the same assay with RA-DEVD-B and GA gave similar results, albeit with opposite color changes (Supplementary Fig. 2).

To investigate whether FPX could be performed between two different cellular compartments, we performed imaging of apoptotic cells co-expressing ^{NES}RA-DEVD-B^{NLS} and GA^{NLS}, where NES represents a genetically fused nuclear export signal[8] and NLS represents a fused nuclear localization sequence[9] (Fig. 1e). Red fluorescence, initially

dispersed through both the nucleus and cytoplasm, was lost upon activation of caspase-3 due to liberation of B^{NLS} from RA. Translocation of B^{NLS} to the nucleus led to formation of a heterodimer with GA^{NLS}, and an increase in green fluorescence (Fig. 1fg, Supplementary Fig. 3, and Supplementary Movie 2). Analogous results were obtained with GA^{NES}-DEVD-B^{NLS} and RA^{NLS} (Supplementary Fig. 4 and Supplementary Movie 3). A compelling feature of the translocating FPX caspase biosensors is that the accumulation of the second color in the nucleus could be useful for long-term monitoring of low levels of protease activity. To demonstrate this application, we used GA^{NES}-DEVD-B^{NLS} and RA^{NLS} to monitor caspase-3-dependent neuritic pruning in cultured rat hippocampal neurons depleted of nerve growth factor (Supplementary Fig. 5, 6)[10]. Having demonstrated that the B copy could be exchanged, we next demonstrated that an A copy could be exchanged between a B copy in the cytoplasm and a B copy in the nucleus (Supplementary Figs. 7-9). Attempts to perform translocation of the A copy from the nucleus to cytoplasm were not successful (Supplementary Fig. 10).

To determine if FPX technology could be used to image dynamic and reversible protein-protein interactions, we applied the technology to the Ca^{2+}-dependent interaction of calmodulin (CaM) and the Ca^{2+}-CaM interacting peptide M13 (Fig. 2a). Fluorescence imaging of HeLa cells transfected with genes encoding RA-CaM, M13-B, and free GA revealed that histamine stimulated Ca^{2+} oscillations were associated with increases in red, and decreases in green, fluorescence (Fig. 2bc and Supplementary Movie 7). To explore the utility of this approach for imaging of other signaling processes, we created biosensors for phosphatidylinositol 4,5-bisphosphate (PIP_2) hydrolysis, protein kinase A (PKA) activation, and Extracellular signal Regulated Kinase (ERK) activity. To image PIP_2 hydrolysis, we co-expressed RA fused to a plekstrin homology (PH) domain, B fused to PH domain, and GA (Fig. 2d). Cells initially exhibited red fluorescence on the plasma membrane, consistent with a high effective concentration of RA and B subunits, and green fluorescence throughout the cytoplasm due to an excess of the B-PH fusion. Stimulation with carbachol led to loss of red fluorescence on the membrane and a whole cell increase in green-to-red ratio (Fig. 2e, Supplementary Fig. 11a and Supplementary Movie 8). To image PKA activation, we co-expressed RA fused to the PKA catalytic domain, B fused to the PKA regulatory domain, and free cytosolic GA (Fig. 2f). Treatment with isoproterenol to stimulate elevation of cAMP and dissociation of the catalytic and regulatory domains produced an increase in the green-to-red ratio (Fig. 2g, Supplementary Fig. 11b). To create an FPX-based biosensor of ERK activity, we replaced YPet and ECFP of the FRET-based EKARev biosensor[11] with RA and B, respectively, and co-expressed this construct with GA^{NES}. Ratiometric responses comparable to those with EKARev (~50%), were observed following treatment with epidermal growth factor (Supplementary Fig. 12ab).

We reasoned that it might be possible to combine all three components of the FPX system into a single polypeptide chain to simplify the transfection procedure while also substantially decreasing the high cell-to-cell variability in expression levels and fluorescence ratios associated with the intermolecular approach. To test this idea, we constructed a tripartite single polypeptide Ca^{2+} biosensor with the structure RA-CaM-B-M13-GA (Fig. 3a). In this arrangement, we presume that the protein exists as an equilibrium mixture in which B is sometimes associated with RA and sometimes with GA. While we could not

predict in advance if this equilibrium would favor the red or green state, we were confident that Ca^{2+}-dependent association of CaM and M13 would perturb the equilibrium. Indeed, we observed that the red-to-green ratio was initially ∼3 and this increased to ∼4 in response to histamine-induced Ca^{2+} oscillations (Fig. 3bc and Supplementary Movie 9). Photobleaching of the red state was more pronounced for the single polypeptide Ca^{2+} biosensor than for the intermolecular Ca^{2+} biosensor (Fig. 2abc). We reason that the intermolecular design benefits from exchange with the large pool of unbound RA (and GA) monomers that are in a dark, quenched, state and thereby protected from photobleaching. Notably, for both the inter- and intramolecular FPX strategies, a useful ratiometric biosensor was created on the first attempt, supporting the idea that FPX is relatively insensitive to linker length and composition. In contrast, 28 designs were tested during the development of cameleon-1, the first FRET-based Ca^{2+} biosensor[12].

To determine if single polypeptide FPX constructs could also be applied to protease activity biosensing, we constructed RA-linker-B-DEVD-GA^{NES} (Fig. 3d). We expected this construct to initially exhibit a combination of green and red fluorescence due to intramolecular exchange of the B copy between the two A copies. Upon cleavage, GA would be released and RA would preferentially bind with B. Imaging of transfected cells undergoing apoptosis revealed a consistent baseline ratio and a pronounced increase in red-to-green ratio upon caspase cleavage (Fig. 3ef and Supplementary Movie 10). Analogous experiments for imaging of caspase-8 activity (RA-IETD-B-linker-GA^{NES}) with release of RA led to the expected increase in green-to-red ratio (Supplementary Fig. 13 and Supplementary Movie 11). To demonstrate the practical utility of this design, we constructed a caspase-1 biosensor (RA-linker-B-YVAD-GA) and used it as a marker of pro-inflammatory processes and pyroptotic cell death[13] in three cell lines exposed to inflammatory and non-inflammatory stimuli (Supplementary Fig. 14). A tripartite construct containing both caspase-8 and caspase-3 substrates (i.e., RA-IETD-B-DEVD-GA^{NES}) gave a decrease in green-to-red ratio during apoptosis (Supplementary Fig. 15). However, the very high levels of caspase-3 activity (Fig. 3f) relative to caspase-8 activity (Supplementary Fig. 13c) complicated the interpretation of these results.

We have demonstrated the versatility of the FPX biosensing strategy by applying it in a variety of live cell imaging applications. A limitation of FPX is that it is not suitable for quantitative imaging due to complications arising from variable protein expression levels (for intermolecular applications) and the inherent and differing affinities of GA and RA for the B copy. In applications where quantitation is not required, FPX minimizes the need for extensive biosensor optimization and provides a versatile new approach to building the next generation of biosensors.

Online Methods

General Methods and Materials

All synthetic DNA oligonucleotides were purchased from Integrated DNA Technologies. Pfu polymerase (Thermo scientific) was used for standard PCR reactions. PCR products and products of restriction digests were purified by gel electrophoresis and extracted by GeneJET gel extraction kit (Thermo scientific) according to the manufacturer's protocols.

Restriction enzymes were purchased from New England Biolabs or Thermo Scientific. Site-directed mutagenesis was performed using Quikchange Lightning kit (Agilent), following the manufacturer's instruction. The cDNA sequences were confirmed by dye terminator cycle sequencing using the BigDye Terminator v3.1 Cycle Sequencing kit (Life Technologies). Sequencing reactions were analyzed at the University of Alberta Molecular Biology Service Unit. Cultured cells were not tested for the presence of *Mycoplasma*, as such contamination would not impact the conclusions made on the basis of our imaging results. The sequences of all primers are provided in Supplementary Table 2.

Protein purification and *in vitro* characterization

For expression and purification of A and B copy proteins, the genes were subcloned into pBAD/His B, and the resulting plasmids were used to transform ElectroMax DH10B *E. coli* (Life Technologies). Single colonies were used to inoculate TB broth supplemented with 100 mg/L ampicillin. After 2 h, 0.02% L-arabinose was added to induce protein expression. Cultures were then further incubated at 30°C for 15-20 h. Cells were harvested by centrifugation at 7000 rpm for 10 min (Beckman), re-suspended in Tris-Cl buffer (pH 7.4), and lysed using a high pressure homogenizer (Constant System Ltd.) under 20 Kpsi. His-tagged soluble proteins were purified from cleared cell lysate by nickel-NTA resin (MCLAB). The lysate-resin mixture was transferred to a column and rinsed with wash buffer (50 mM Tris-HCl, 300 mM NaCl, 20 mM imidazole, pH 8.0). Proteins were then eluted from the resin using 50 mM Tris-Cl (pH 7.4) supplemented with 300 mM NaCl and 300 mM imidazole. Proteins were concentrated and buffer exchanged into Tris-Cl buffer (pH 7.4) using a centrifugal filter devices with a 10 kDa MWCO (EMD Millipore). Finally, a BCA assay and SDS-PAGE analysis were performed to determine protein concentration and confirm the purity.

For *in vitro* measurements of the dissociation constant (K_d) of various AB heterodimers, increasing amounts of the non-fluorescent B copy were added to a fixed amount of A copy, thereby generating a fluorescent AB complex. Fluorescence emission spectra were recorded using a QuantaMaster spectrofluorometer (Photon Technology International, Inc.). Saturation binding curves were generated by plotting the integrated fluorescence emission intensity as a function of B copy concentration. Experimental data were fit using the Langmuir equation (Origin 9.0).

For *in vitro* measurements of caspase-3 activity in neurons, proteins were extracted in caspase lysis buffer (50 mM HEPES, pH 7.4, 0.1% 3-([3-cholamidopropyl]dimethylammonio)-1-propanesulfonate (CHAPS), 1 mM DTT, and 0.1 mM EDTA) for 10 min on ice followed by microcentrifugation to remove insoluble material. Protein concentration was determined by BCA assay (Pierce). Proteins (10 μg per 100 μL reaction assay) were added to 10 ng of recombinant active caspase (PharMingen) in assay buffer (20 mM PIPES, 30 mM NaCl, 10 mM DTT, 1 mM EDTA, 0.1% CHAPS, and 10% sucrose, pH 7.2) and 68.5 μM acetylated (Ac)-DEVD-7-amino-4-trifluoromethyl coumarin (AFC) for caspase-3. The caspase-3 activity was measured at 37°C every 2 min for 1 hr to determine the linear range of activity. Based on an AFC standard curve, the

amount of released AFC was measured and the specific activity of the caspase-3 was determined as nanomoles of released AFC per microgram of protein per minute[14].

Assembly of reporter gene plasmids

DNA encoding a nuclear exclusion sequence (NES; sequence LALKLAGLDIGS)[8] or a triplicate copy of a nuclear localization sequence (NLS; sequence DPKKKRKVDPKKKRKVDPKKKRKV)[9] was appended to either the 5′ or 3′ end of the gene of copy A or B to construct the fusions described in Supplementary Table 1. The gene sequences encoding A^{NES}, A^{NLS}, B^{NES}, or B^{NLS} were PCR amplified with primers containing a 5′ XhoI site and a 3′ KpnI site, or a set of primers containing a 3′ HindIII site and a 5′ KpnI site followed by a sequence encoding HSTHSHSSHTASHDEVDGA. The tandem heterodimer construct was built by ligating XhoI/KpnI digested fusions with KpnI/HindIII digested DEVD containing fusions into pcDNA3.1(+) (Life Technologies) with a three-part ligation. Tandem ddFP heterodimers for caspase-8 and caspase-9 biosensors were constructed in the same manner, except the DEVD sequence was replaced by IETD and LEHD sequence, respectively. To construct A^{NES}, A^{NLS}, B^{NES}, or B^{NLS}, the appropriate gene regions were amplified using primers encoding a 5′ XhoI site and a 3′ HindIII site. The XhoI/HindIII digested fusions were then ligated into pcDNA3.1(+) cut with the same two enzymes. For the one plasmid dual caspase biosensor, RA-IETD-B-DEVD-GA^{NES}, two gene fragments and a HindIII and XhoI digested vector pcDNA3.1(+) were assembled in a three-part ligation. A previously created caspase-8 biosensor, containing a RA-B heterodimer with a duplicated IETD sequence as linker, was used as template for the first fragment. A 5′ primer containing a HindIII site, and a 3′ primer containing a BamHI site, were used to amplify the first fragment HindIII-RA-KpnI-2×IETD-B-BamHI. The second fragment was created by amplifying GA-NES using a 5′ primer containing a BamHI site and a sequence encoding the DEVD substrate sequence, and a 3′ primer containing an XhoI site. The single plasmid caspase-3 biosensor, RA-linker-B-DEVD-GA^{NES}, was created by performing site-directed mutagenesis on RA-IETD-B-DEVD-GA^{NES} to replace the sequence encoding duplicated IETD with a linker sequence encoding an XhoI site. This additional site was used to facilitate rapid screening of ligation products by diagnostic analytical digestion. Similarly, the single plasmid caspase-8 biosensor, RA-IETD-B-linker-GA^{NES}, was created by performing site-directed mutagenesis on RA-IETD-B-DEVD-GA^{NES} to replace the DEVD sequence with a linker encoding a KpnI site.

To construct the caspase-1 biosensor, RA-linker-B-YVAD-GA, GA was PCR amplified using a 5′ primer containing BamHI site and sequence encoding three repeats of caspase-1 substrate YVAD, and a 3′ primer containing a XhoI site. The BamHI/XhoI digested PCR product was then ligated together with HindIII/BamHI digested RA-linker-B-DEVD-GA^{NES} and HindIII/XhoI digested pcDNA3.1 (+). For caspase-1 activity imaging, plasmids were prepared in α-Select *E. coli* (Bioline) and isolated by Miniprep kit (Qiagen). DNA concentration was adjusted to 1 μg/μl in purified water, and plasmids were stored at -20°C.

For the intermolecular Ca^{2+} biosensor, the previously reported RA-CaM and M13-B constructs were used[6]. GA^{NES} was prepared as described above. A three-part ligation was used to construct the gene encoding the intramolecular (single plasmid) Ca^{2+} biosensor, RA-

CaM-B-M13-GA^{NES}. The first fragment was amplified from template RA-CaM with primers containing a 5′ XhoI site and a 3′ BamHI site. The second fragment, B-M13-GA, was created by first replacing B with GA from construct M13-B to construct M13-GA. Subsequently, M13-GA was amplified with primers containing a 5′ EcoRI site and a 3′ HindIII site and then digested with EcoRI. A B copy was amplified with primers containing a 5′ BamHI and a 3′ EcoRI site, and then digested with EcoRI. These two EcoRI-digested fragments were ligated, digested with BamHI/HindIII, and the resulting fragment was used in a three-part ligation with the digested first fragment and XhoI/HindIII digested pcDNA3.1(+).

To construct the PIP_2 biosensor, genes encoding RA and B were ligated to the 5′ end of the pleckstrin homology (PH) domain of PLCδ (amplified from Addgene plasmid 21262)[15]. The ligation product was inserted into a modified pcDNA3.1 using the In-Fusion Cloning kit (Clontech) To construct the cAMP-dependent PKA biosensor, the gene encoding RA was fused to the 5′ end of the catalytic subunit of PKA, and the gene encoding B was fused to the 3′ end of the regulatory subunit. Plasmids encoding the catalytic and regulatory subunits of PKA were obtained from Origene (MC200197) and Source Bioscience (IRATp970F0898D), respectively. Ligation products were separately cloned into modified pcDNA3.1 with the In-Fusion Cloning kit (Clontech).

The gene construct for the ERK biosensor was assembled in a pcDNA3.0 vector with a modified multiple cloning site. The modified EKARev[11] with RA and B was cloned via two steps. In the first step, the RA fragment containing a short linker flanked by a BglII/KpnI at its 3′ end was generated and ligated to a PCR-generated B fragment using the sites KpnI/EcoRI together in a linearized pRSET-B vector, forming a tandem RA-B construct. Replacing the short linker within the tandem construct with a PCR-generated fragment containing the EKARev phosphorylation-responsive domain through the sites BglII/KpnI yielded the desired product. The constructs were then subcloned into linearized pcDNA3.0 via the BamHI/EcoRI sites

Cell culture and transfection

HeLa cells used for caspase-3, caspase-8, caspase-9, and Ca^{2+} imaging experiments were maintained in Dulbecco's Modified Eagle Medium (DMEM) supplemented with 10% fetal bovine serum (FBS) and Glutamax (Life Technologies) at 37°C and 5% CO_2. Transient transfections of pcDNA3.1(+) expression plasmids were performed using Turbofect (Thermo Scientific). HeLa cells in 35 mm imaging dishes were incubated with 1 mL of DMEM (FBS free) for 10 min and then transfected with 1 μg of plasmid DNA that had been mixed with 2 μL of Turbofect (Thermo Scientific) in 0.1 mL of DMEM (FBS free). The culture media was changed back to DMEM with 10% FBS after 2 h incubation at 37°C.

For imaging of caspase-3 activity in neurons, rat primary neurons were cultured from newborn Sprague Dawley (SD) rat hippocampus and mouse primary neurons were cultured from the hippocampus following the regulations of Peking University Animal Care and Use Committee[16]. In brief, fresh rat hippocampal tissues were dissociated with 0.25% trypsin (Life Technologies), which was then inactivated by 10% decomplemented FBS (Thermo Scientific). The mixture was triturated through pipette to make a homogenous mixture. After

filtering the mixture through 70 μm sterilized filters, the flow-through was centrifuged. The pellet was then washed once by PBS and once by DMEM containing 0.225% sodium bicarbonate, 1 mM sodium pyruvate, 2 mM L-glutamine, 0.1% dextrose, 1× Penicillin-Streptomycin (Life Technologies) with 5% FBS. Cells were then plated on poly-L-lysine (Sigma) coated plates or glass coverslips at the density of 3×10^6 cells/ml. Neurons were incubated at 37°C in DMEM without phenol red with 5% FBS and 5% CO_2. Cytarabine was added to culture media 24 h after plating at 10 μM to inhibit cell growth. Medium was changed every 48 h. Thin-walled borosilicate glass capillaries (outer diameter = 1.0 mm, inner diameter = 0.5 mm) with microfilament (MTW100F-4, World Precision Instrument) were pulled with a Flaming/Brown Micropipette Puller (P-97, Sutter) to obtain injection needles with a tip diameter of ∼0.5 m. Microinjections were performed in the cytosol of each cell using the Eppendorf Microinjector FemtoJet and Eppendorf Micromanipulator (Eppendorf). Neurons were injected with 25 fl/shot at an injection pressure of 100 hPa, a compensation pressure of 50 hPa, and an injection time of 0.1 seconds. GA^{NES}-DEVD-B^{NLS} and RA^{NLS} were injected into the cytosol at 30 ng/ml. Approximately 90% neurons survive the injections for at least 16 days[17].

For imaging of PIP_2 and PKA activities, HEK293 cells were cultured in Eagle's minimal essential medium (EMEM, ATCC) supplemented with 10% FBS and penicillin-streptomycin (Life Technologies) at 37°C in a 5% CO_2 atmosphere. Prior to cell seeding, 96-well glass-bottom plates were coated with poly-D-lysine (Fisher Scientific). Cells were seeded and transfected using Lipofectamine 2000 (Life Technologies) according to the manufacturer's protocol, and incubated for 30 to 48 h at 37°C in 5% CO_2. For PIP_2 imaging, HEK293 cells were cotransfected with the DNA vector encoding the PIP_2 biosensor (50 ng), plus the vector encoding GA (50 ng), plus a vector (30 ng) encoding human M1 muscarinic acetylcholine receptor (M1 mAChR). For PKA imaging, cells were transfected with the vector encoding the PKA biosensor (50 ng), plus the vector encoding GA (50 ng), and a vector (30 ng) encoding the rat beta-adrenergic receptor (βAR). Vectors encoding M1 mAChR and βAR were obtained from the Missouri S&T cDNA Resource Center (www.cdna.org).

For imaging of ERK activity, HEK293 cells were maintained in DMEM growth media supplemented with 10% FBS, 1% penicillin and streptomycin. All cells were transfected at an approximate confluency of 70% using Lipofectamine 2000 reagent and incubated for 24 h before imaging. All cells were imaged in Hank's balanced salt solution (HBSS) buffer at room temperature.

For caspase-1 activity imaging, the MCF-7, U251 and HepG2 cell lines were obtained from the American Type Culture Collection. Unless otherwise specified, MCF-7 and U251 cells were cultured in DMEM and HepG2 cells were cultured in minimum essential media (MEM) containing 10% FBS, 2 mM L-glutamine, 100 IU/mL penicillin, 100 μg/mL streptomycin (Life Technologies), and 1% non-essential amino acids. Cells were incubated at 37°C with 5% CO_2. Cells were seeded in black 96-well plates (Corning) at a density of 10,000 cells per well, and cultured for 24 h. Transfection was conducted in the absence of antibiotics, using Lipofectamine 2000 (Life Technologies), following the procedure recommended by the manufacturer. The transfection complexes were kept for 12 h, after

which the medium was refreshed, and cells were allowed to recover for another 12 h before treatment.

Cell treatments and imaging conditions

Transfected HeLa cells were imaged using an Axiovert 200M (Zeiss), or a laser scanning confocal LSM-700 (Zeiss), or a Nikon Eclipse Ti. The Axiovert 200M (Zeiss) was equipped with a 75 W xenon-arc lamp, a 40× objective lens (NA = 1.3, oil), a 14-bit CoolSnap HQ2 cooled CCD camera (Photometrics), and was driven by open source Micro-Manager software. The LSM-700 (Zeiss) was equipped with 10 mW 488 nm and 555 nm solid-state laser, 63× objective lens (NA = 1.40, oil), two high-sensitivity, low-noise adjustable PMTs, and was driven by Zeiss's Zen software. The Nikon Eclipse Ti microscope was equipped with a 150 W Lumen 200 metal halide lamp (Prior Scientific), a 16-bit 512SC QuantEM CCD (Photometrics), a 25% neutral density filter, a 40× objective (NA = 0.95, air), and was driven by a NIS-Elements AR 3.0 software package (Nikon).

For imaging of caspase-3, caspase-8, and caspase-9 activities imaging in HeLa cells, apoptosis was initiated by treatment with 2 μM staurosporine at 24 to 48 h post-transfection. Cells were maintained in HEPES-buffered HBSS (HHBSS) and subjected to imaging at 1 or 2 min intervals for 4-6 h. For imaging of Ca^{2+} concentration dynamics in HeLa cells, transfected cells were imaged in HHBSS and were consecutively treated with histamine (0.1 mM) in Ca^{2+} free HHBSS, EGTA (10 mM) in Ca^{2+} free HHBSS with ionomycin (5 μM), and $CaCl_2$ (10 mM) in HHBSS with ionomycin (5 μM), Images were acquired at 5 s or 10 s intervals for up to 60 minutes, using an inverted Nikon Eclipse Ti microscope as described above. All cell images were processed and analyzed using ImageJ (http://imagej.nih.gov/ij/). All intensity and ratio traces were plotted as scatter charts with smoothed lines in Microsoft Excel.

For imaging of the PIP_2 biosensor and the cAMP biosensor, EMEM culture medium was replaced with 1× Dulbecco's phosphate-buffered saline (DPBS) prior to live cell imaging. A Zeiss Axiovert S100TV inverted microscope equipped with computer-controlled excitation and emission filter wheels, shutters, and a Qimaging Retiga Exi CCD camera was used to image cells at 25 °C using the 10× objective lens (N.A. 0.3). Red fluorescence was detected with 572/20 nm excitation and 630/30 nm emission filters. Green fluorescence was detected with 480/20 nm excitation and 535/25 nm emission filters. To analyze the image stacks, background fluorescence was defined as a region of the image that contained no cells. The average value of the background region was subtracted frame by frame from measurements of the mean pixel values from cells. Red and green fluorescence measured before and after addition of an agonist to activate the co-expressed receptor. PIP_2 activation was done by the addition of 50 μM carbachol (Sigma). PKA activation was done by the addition of 50 μM isoproterenol (Sigma).

For imaging of caspase-3 activity during neuritic pruning, cell treatments for experiments were performed after 7 days in culture. Nuclear fluorescence intensity of live cells was measured with ImageJ by limiting the region of interest (ROI) to the area defined by Hoechst nuclear staining. Staurosporine (Sigma) was added to the culture medium to a final concentration of 5 μM. After a 6 h treatment, the neurons were subject to imaging for 2 h.

NGF-free medium with 1:20000 dilution of 23c4 anti-NGF neutralizing antibody[18] was added to the neurons for 24 h before the images were taken. The nuclei were co-stained by Hoechst 33342 (1 μg/ml, Sigma). The nuclear fragmentation was analyzed with a fluorescence Live Cell Imaging microscope (Olympus) by counting the number of fragmented nucleus out of a total of 100 nuclei in each treatment group.

Epifluorescence imaging of ERK activity was performed on a Zeiss Axiovert 200M Microscope equipped with a Xeon lamp and a cooled CCD, under a 40× oil immersion objective. Ratiometric fluorescence imaging of FPX biosensors was performed using a 480/30 nm excitation filter and a 535/45 nm emission filter for green fluorescence, and a 568/55 nm excitation filter and 653/95 nm emission filter for red fluorescence. All epifluorescence experiments were subsequently analyzed using the MetaFluor software (Molecular Devices).

For caspase-1 activity imaging, culture medium was refreshed before treatment. *E. coli* lipopolysaccharide (1 μg/mL; LPS; Sigma-Aldrich), adenoside triphosphate (5 mM; ATP; Sigma-Aldrich), tumor necrosis factor alpha (10 ng/mL; TNF-α; Sigma-Aldrich), palmitic acid (100 μM; Sigma-Aldrich) and ethanol (50 mM; Fisher) stocks were prepared in purified water. Staurosporine (0.5 μM; STS; Sigma-Aldrich) and curcumin (10 μM; CUR; Sigma-Aldrich) were diluted in dimethyl sulfoxide (DMSO). DMSO in-well concentration was kept below 0.1%. Treatment was maintained for 4 h in complete medium, after which cells were imaged using fluorescence microscopy. An automated platform (Operetta High Content Imaging System; Perkin Elmer) was used to image cells displaying green (eGFP) and red (Alexa 594) signals. Caspase-1 activity was quantified as the whole cell ratio of red-to-green fluorescence. Eleven fields were analyzed per well, with six wells per condition. Non-transfected cells were used as negative controls, in the presence or absence of drugs.

Statistical analysis

For analysis of caspase-3 activity in neurons, statistical significance was assessed by one-way analysis of variances (ANOVA). The Sheffé's test was applied as a *post hoc* for the significant difference showed by ANOVAs. A p value of less than 0.05 was used as an indicative of statistical significance. Power analysis for each experiment to validate group size was done by SPSS V13.0.

For caspase-1 activity imaging, at least three independent experiments were performed for each condition, and each condition was included in sixplicate. All data are expressed as mean ± SEM. The Student's *t*-test with Bonferroni correction was used to analyze significant differences between group means (p values < 0.01 were considered to be significant).

Supplementary Material

Refer to Web version on PubMed Central for supplementary material.

Acknowledgments

We thank the University of Alberta Molecular Biology Service Unit, C.W. Cairo and R. Derda for technical assistance, T. Meyer (Stanford) for the PLCδ gene, and anonymous peer reviewers for their valuable guidance.

Funding support provided by Alberta Glycomics Centre (R.E.C), Canadian Institutes of Health Research (NHG 99085 and MOP 123514 to R.E.C. and MOP 119425 to D.M.), Natural Sciences and Engineering Research Council of Canada (Discovery grant to R.E.C. and a CGSD3 Scholarship to S.C.A), Alberta Ingenuity Ph.D. Scholarships (S.C.A. and Y.S.), a National Science Foundation of China Major Research Grant (91132718 to Y.Z.), Beijing Natural Science Foundation (7142085 to Y.Z.), US National Institutes of Health DP1 CA174423 (to J.Z.), and US National Science Foundation Small Business Innovation Research (SBIR) 1248138 and Montana SBIR matching funds #13-50 RCSBIR-003 (A.M.Q). R.E.C. held a Tier II Canada Research chair.

References

1. Miyawaki A, et al. Nature. 1997; 388:882–887. [PubMed: 9278050]
2. Xu X, et al. Nucleic Acids Res. 1998; 26:2034–2035. [PubMed: 9518501]
3. Hu CD, Chinenov Y, Kerppola TK. Mol Cell. 2002; 9:789–798. [PubMed: 11983170]
4. Nagai T, Sawano A, Park ES, Miyawaki A. Proc Natl Acad Sci U S A. 2001; 98:3197–3202. [PubMed: 11248055]
5. Nakai J, Ohkura M, Imoto K. Nat Biotechnol. 2001; 19:137–141. [PubMed: 11175727]
6. Alford SC, Abdelfattah AS, Ding Y, Campbell RE. Chem Biol. 2012; 19:353–360. [PubMed: 22444590]
7. Alford SC, Ding Y, Simmen T, Campbell RE. ACS Synth Biol. 2012; 1:569–575. [PubMed: 23656278]
8. Wen W, Meinkotht JL, Tsien RY, Taylor SS. Cell. 1995; 82:463–473. [PubMed: 7634336]
9. Kalderon D, Roberts BL, Richardson WD, Smith AE. Cell. 1984; 39:499–509. [PubMed: 6096007]
10. Simon DJ, et al. J Neurosci. 2012; 32:17540–17553. [PubMed: 23223278]
11. Komatsu N, et al. Mol Biol Cell. 2011; 22:4647–4656. [PubMed: 21976697]
12. Miyawaki A, Tsien RY. Methods Enzymol. 2000; 327:472–500. [PubMed: 11045004]
13. Bergsbaken T, Fink SL, Cookson BT. Nat Rev Microbiol. 2009; 7:99–109. [PubMed: 19148178]

References for Online Methods

14. Zhang Y, Tounekti O, Akerman B, Goodyer CG, LeBlanc A. J Neurosci. 2001; 21:RC176. [PubMed: 11588206]
15. Botelho RJ, et al. J Cell Biol. 2000; 151:1353–1368. [PubMed: 11134066]
16. Cui J, et al. J Neurosci. 2011; 31:16227–16240. [PubMed: 22072674]
17. LeBlanc A. J Neurosci. 1995; 15:7837–7846. [PubMed: 8613723]
18. Weskamp G, Otten U. J Neurochem. 1987; 48:1779–1786. [PubMed: 3572400]

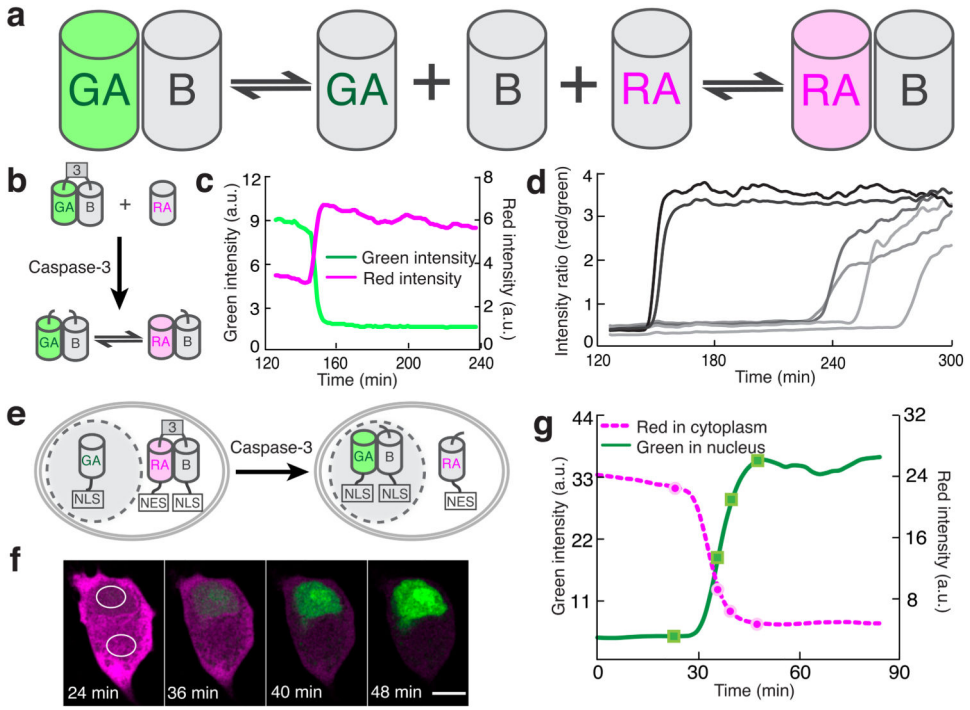

Figure 1.

The FPX strategy and application to imaging of protease activity. (**a**) Schematic overview of the FPX strategy. (**b**) Green-to-red FPX detection of caspase-3 activity. See Supplementary Table 1 for construct details. (**c**) Green and red whole cell intensities vs. time for a HeLa cell co-expressing GA-DEVD-B and RA and undergoing apoptosis. X-axis for all caspase activity imaging traces is time elapsed since 1 h after treatment with staurosporine. (**d**) Whole cell red-to-green intensity ratios vs. time (average ratio change = 7.8 ± 0.9-fold (n = 6)) for multiple cells treated and analyzed as in (**c**). (**e**) A red-to-green FPX protease biosensor based on translocation of the dark B copy. (**f**) Selected merged frames (see Supplementary Movie 2) from two-color imaging of staurosporine-treated HeLa cells co-expressing ^{NES}RA-DEVD-B^{NLS} and GA^{NLS}. Red fluorescence is represented as magenta. Scale bar represents 10 μm. (**g**) Intensity vs. time for the regions of interest (ROIs) indicated in (**f**).

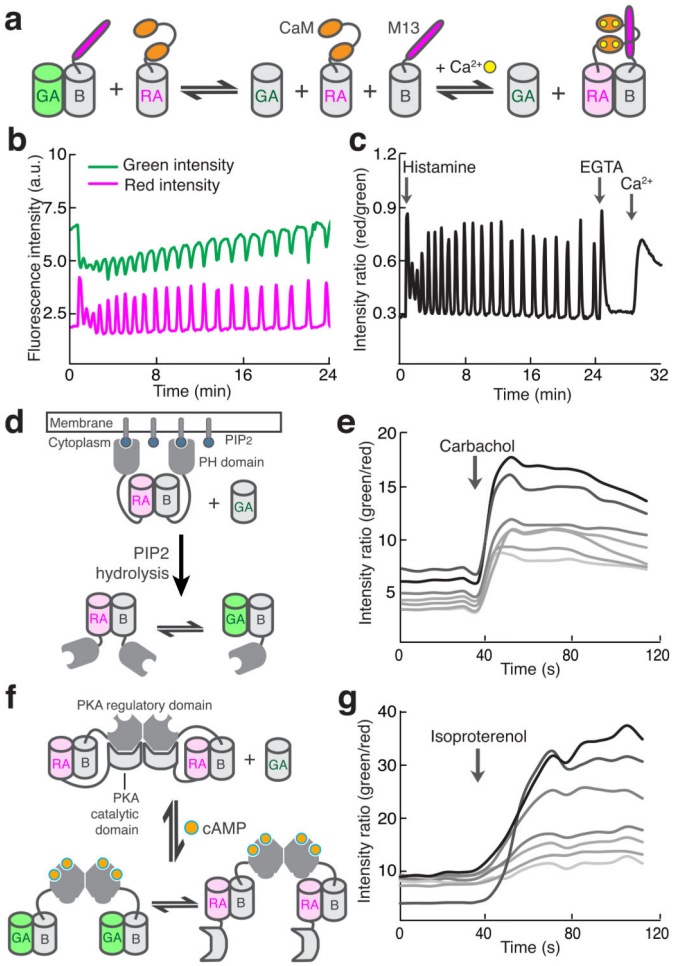

Figure 2.

Intermolecular FPX for imaging of second messenger signaling. (**a**) Schematic representation of using FPX technology for imaging of the Ca^{2+}-dependent interaction of CaM and the Ca^{2+}-CaM interacting peptide M13. (**b**) The intensity in the green and red emission channels for a representative HeLa cell (n = 12) treated with histamine. (**c**) The ratio of the red-to-green signals for the same cell as in (**b**). Maximum red-to-green ratio changes due to histamine treatment = 3.2 ± 0.7-fold (n = 7). (**d**) Schematic representation of FPX for imaging of PIP_2 hydrolysis to generate diacylglycerol and inositol 1,4,5-trisphosphate (IP_3). (**e**) Green-to-red ratio vs. time for 7 cells expressing genes encoding the proteins represented in (**d**) and treated with carbachol. (**f**) Schematic representation of FPX for imaging of cAMP-dependent protein kinase A (PKA) activation. (**g**) Green-to-red ratio vs. time for 7 individual cells expressing genes encoding the proteins represented in (**f**) and treated with isoproterenol.

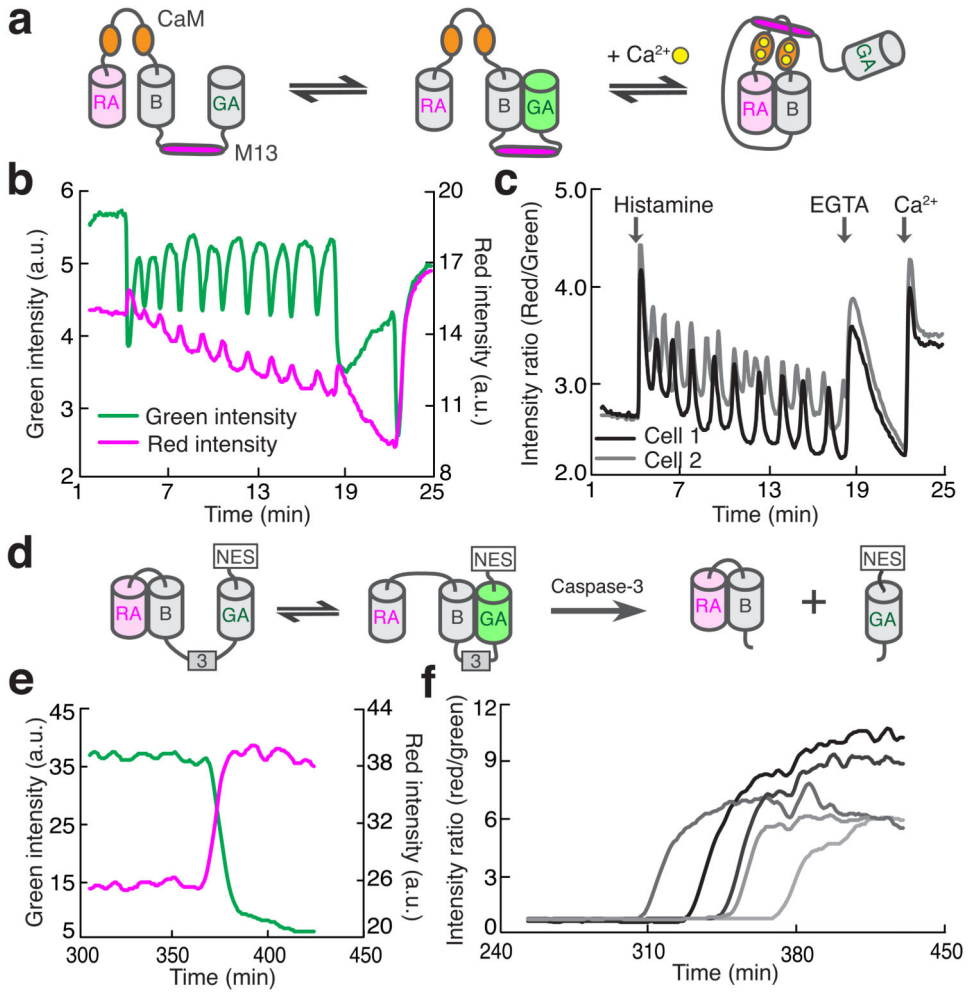

Figure 3.

Intramolecular FPX using tripartite single polypeptides. (**a**) Schematic representation of a single polypeptide FPX biosensor for Ca^{2+}. (**b**) Intensity vs. time of green and red fluorescence for a representative HeLa cell (n = 18) expressing RA-CaM-B-M13-GA and undergoing histamine-induced Ca^{2+} oscillations. (**c**) Red-to-green ratio vs. time for the cell represented in (**b**) (cell 1) and a second cell (cell 2). (**d**) Schematic representation of single polypeptide FPX for imaging of caspase-3 activity. (**e**) Whole cell green and red intensities for a HeLa cell expressing RA-linker-B-DEVD-GA^{NES} and undergoing staurosporine-induced apoptosis. (**f**) Red-to-green intensity ratio vs. time for multiple cells expressing the construct shown in (**d**). The average red-to-green ratio change = 10 ± 5-fold (n = 5).